ChemComm

COMMUNICATION

View Article Online
View Journal | View Issue

Cite this: *Chem. Commun.*, 2016, 52, 4171

Received 15th December 2015,
Accepted 17th February 2016

DOI: 10.1039/c5cc10311h

www.rsc.org/chemcomm

Highly efficient hydrogen generation from formic acid using a reduced graphene oxide-supported AuPd nanoparticle catalyst†

Xinchun Yang,[ab] Pradip Pachfule,[a] Yao Chen,[a] Nobuko Tsumori[c] and Qiang Xu*[ab]

Highly dispersed AuPd alloy nanoparticles have been successfully immobilized on reduced graphene oxide (rGO) using a facile non-noble metal sacrificial method, which exhibit the highest activity at 323 K (turnover frequency, 4840 h^{-1}) for hydrogen generation without CO impurity from the formic acid/sodium formate system.

Hydrogen is of critical importance in clean energy applications although effective hydrogen storage technologies still need to be developed.[1] Formic acid (FA) is a promising hydrogen carrier,[2] which has several remarkable features such as (a) nontoxicity with high hydrogen content (4.4 wt%), (b) high stability as a liquid at room temperature, and (c) easy synthesis *via* a biomass process, CO_2 reduction or methyl formate hydrolysis.[3] Depending on the catalysts, however, FA can be decomposed in two ways: desirable dehydrogenation ($HCOOH \rightarrow H_2 + CO_2$) and undesirable dehydration ($HCOOH \rightarrow H_2O + CO$), which produces CO impurities that are toxic to the fuel cell catalysts.[4]

So far, homogeneous catalysts have been extensively studied for hydrogen production from FA and very high catalytic activities have been reported.[5] Along with the ongoing progress in FA dehydrogenation using homogeneous systems, heterogeneous catalysts have attracted tremendous attention due to their advantages of easy separation and recycling. A large number of metal nanoparticle (MNP) catalysts have been studied, most of which, however, suffer from severe aggregation and limited catalytic activities.[6]

Herein, we report a highly active AuPd alloy nanoparticle catalyst prepared using a non-noble metal sacrificial approach (NNMSA), which exhibits the highest turnover frequency (TOF) of 4840 h^{-1} at 323 K for hydrogen generation from the FA/sodium formate (SF) system.[7]

Cobalt was used as the sacrificial agent. Amorphous $Co_3(BO_3)_2$ was formed from the reaction between $Co(CH_3COO)_2$ and $NaBH_4$, which can be easily dissolved in H_3PO_4 (Fig. S1 and S2, for details see the ESI†).[8] Graphite oxide (GO) was prepared from graphite using a modified Hummers' method.[9] The rGO-supported AuPd nanoparticle (NP) catalyst was synthesized using a wet-chemical process, as illustrated in Scheme 1. Firstly, according to the stoichiometry, the aqueous solution containing $HAuCl_4$, $Co(CH_3COO)_2$ and K_2PdCl_4 was added into 50 mL of GO suspension (0.1 wt%). Then the above mixture was reduced by a fresh aqueous solution of $NaBH_4$. After continuous stirring for 2 h, the mixture was washed and re-dispersed in H_3PO_4 solution for etching (2 h). Finally, the catalyst, denoted as $(Co_x)_EAu_yPd_{1-y}$/rGO (ESI†), was obtained by centrifugation and washing with water.

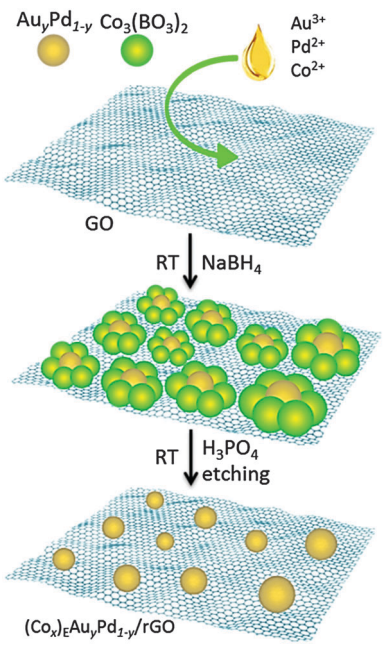

Scheme 1 Schematic illustration of the synthesis of the $(Co_x)_EAu_yPd_{1-y}$/rGO catalyst *via* a non-noble metal (cobalt) sacrificial approach (NNMSA).

[a] *National Institute of Advanced Industrial Science and Technology (AIST), Ikeda, Osaka, Japan. E-mail: q.xu@aist.go.jp, qxuchem@hotmail.com; Fax: +81-72-751-9628; Tel: +81-72-751-9562*
[b] *Graduate School of Engineering, Kobe University, Nada Ku, Kobe, Hyogo, Japan*
[c] *Toyama National College of Technology, 13, Hongo-machi, Toyama, 939-8630, Japan*

† Electronic supplementary information (ESI) available: Experimental procedures, PXRD, TEM, EDX, GC and catalytic activity. See DOI: 10.1039/c5cc10311h

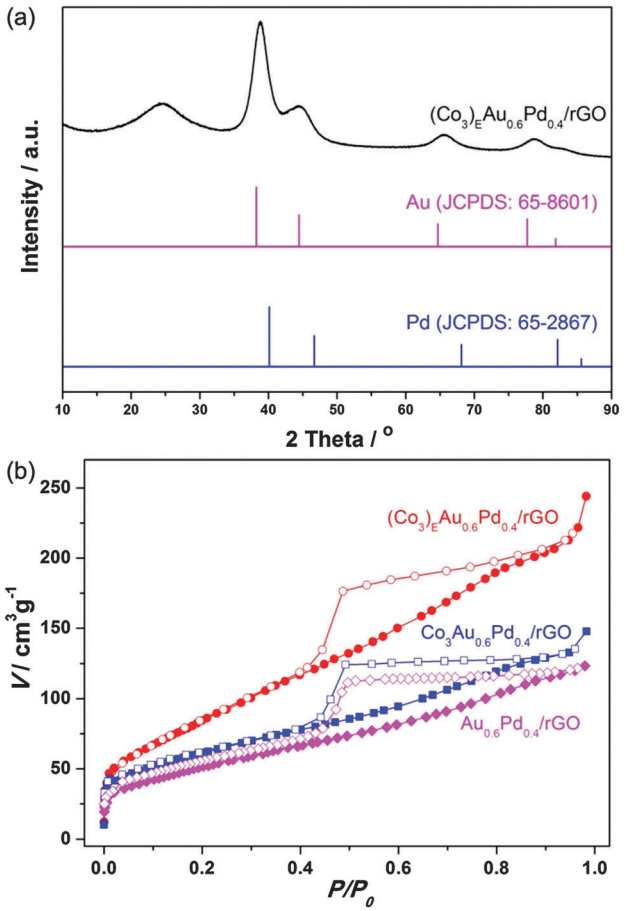

Fig. 1 (a) XRD pattern of $(Co_3)_EAu_{0.6}Pd_{0.4}$/rGO and (b) N_2 sorption analyses (77 K) of $(Co_3)_EAu_{0.6}Pd_{0.4}$/rGO, $Co_3Au_{0.6}Pd_{0.4}$/rGO and $Au_{0.6}Pd_{0.4}$/rGO.

Fig. 1a shows the powder X-ray diffraction (PXRD) pattern of the $(Co_3)_EAu_{0.6}Pd_{0.4}$/rGO catalyst. Except for a low and broad diffraction of rGO at 24°, the diffraction peaks, which are located between the fcc Au (JCPDS No. 65-8601) and Pd (JCPDS No. 65-2867), indicate the formation of an AuPd alloy.[10] For comparison, PXRD patterns of the non-etched counterparts $Co_3Au_{0.6}Pd_{0.4}$ and $Co_3Au_{0.6}Pd_{0.4}$/rGO (Fig. S3, ESI†) show an additional broad band for $Co_3(BO_3)_2$. After etching with an acid, the characteristic peaks corresponding to AuPd are clearly visible and match well with the directly deposited counterpart of $Au_{0.6}Pd_{0.4}$/rGO (Fig. S3, ESI†), confirming the successful removal of cobalt and the formation of AuPd. The N_2 sorption isotherms for $(Co_3)_EAu_{0.6}Pd_{0.4}$/rGO, $Co_3Au_{0.6}Pd_{0.4}$/rGO and $Au_{0.6}Pd_{0.4}$/rGO are shown in Fig. 1b. Generally, the restacking of rGO can be partially overcome by the direct deposition of NPs.[11] Hence, the $Au_{0.6}Pd_{0.4}$/rGO and $Co_3Au_{0.6}Pd_{0.4}$/rGO possess a type-IV N_2 sorption curve with Brunauer–Emmett–Teller (BET) surface areas of 189 and 219 $m^2\ g^{-1}$, respectively. Notably, the surface area of $(Co_3)_EAu_{0.6}Pd_{0.4}$/rGO (321 $m^2\ g^{-1}$) increases drastically, illustrating that the removal of cobalt by the acid etching has resulted in high porosity, which will favour the diffusion of reactants to metal NPs in catalysis.

The morphologies of the $Au_{0.6}Pd_{0.4}$/rGO, $Co_3Au_{0.6}Pd_{0.4}$/rGO and $(Co_3)_EAu_{0.6}Pd_{0.4}$/rGO catalysts were analysed by transmission electron microscopy (TEM). As shown in Fig. S4 and S5 (ESI†), $Au_{0.6}Pd_{0.4}$/rGO and $Co_3Au_{0.6}Pd_{0.4}$/rGO possess larger particles with severe aggregation (ESI†). In contrast, the AuPd NPs in the $(Co_3)_EAu_{0.6}Pd_{0.4}$/rGO catalyst are well dispersed and immobilized on the rGO support (Fig. 2a). The high-angle annular dark-field scanning transmission electron microscopy (HAADF-STEM) images further reveal the uniform distribution of AuPd NPs in the $(Co_3)_EAu_{0.6}Pd_{0.4}$/rGO catalyst with an average particle size of 3.9 ± 0.9 nm (Fig. 2b and c), indicating that the sacrifice of the cobalt compound can prevent the primary AuPd NPs from aggregation, which will benefit their catalytic performance. Energy dispersive X-ray (EDX) analyses (Fig. S6–S8, ESI†) show that $Co_3Au_{0.6}Pd_{0.4}$/rGO is rich in cobalt, whereas no signals for cobalt are detected in $(Co_3)_EAu_{0.6}Pd_{0.4}$/rGO, clearly confirming that cobalt has been eliminated by the H_3PO_4 etching. The inductively coupled plasma optical emission spectroscopic analysis reveals that the molar ratio of Co : Au : Pd in $(Co_3)_EAu_{0.6}Pd_{0.4}$/rGO to be 0.04 : 0.6 : 0.4, indicating that almost all the co-precipitated $Co_3(BO_3)_2$ can be removed by H_3PO_4. The X-ray photoelectron spectroscopic (XPS) measurements show no signals for Co in $(Co_3)_EAu_{0.6}Pd_{0.4}$/rGO before and after Ar sputtering (Fig. 3a). The observed Au 4f and Pd 3d spectra reveals that $(Co_3)_EAu_{0.6}Pd_{0.4}$/rGO is composed of metallic Au and Pd (Fig. 3b and c), further confirming the successful formation of AuPd alloy NPs.

The catalytic activities of the $(Co_x)_EAu_yPd_{1-y}$/rGO catalysts in hydrogen generation from the FA/SF system were evaluated. Fig. 4a shows the gas generation from the FA/SF system in the presence of $(Co_3)_EAu_{0.6}Pd_{0.4}$/rGO and $Au_{0.6}Pd_{0.4}$/rGO. Unquestionably, the sacrificial agent plays a dominant role, by decreasing the size of NPs, in the promotion of catalytic performance. Under our evaluation conditions, the $(Co_3)_EAu_{0.6}Pd_{0.4}$/rGO catalyst shows an extremely high catalytic activity for the complete dehydrogenation

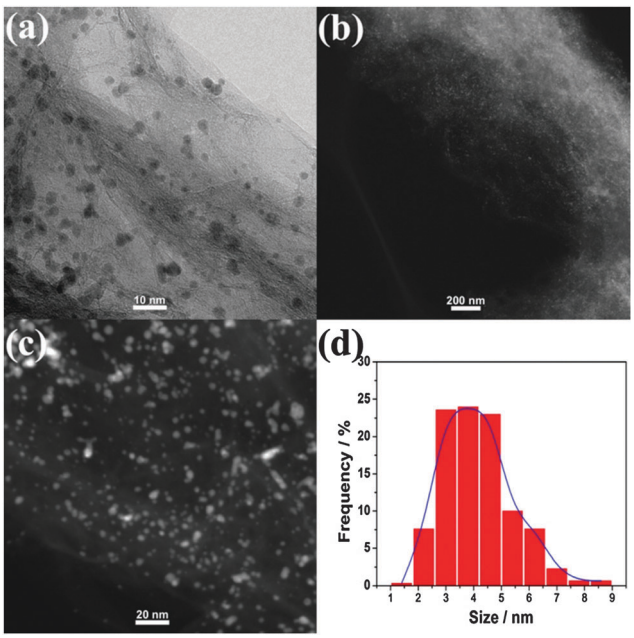

Fig. 2 (a) TEM, (b and c) HAADF-STEM images and (d) particle size distribution histograms of AuPd NPs of $(Co_3)_EAu_{0.6}Pd_{0.4}$/rGO.

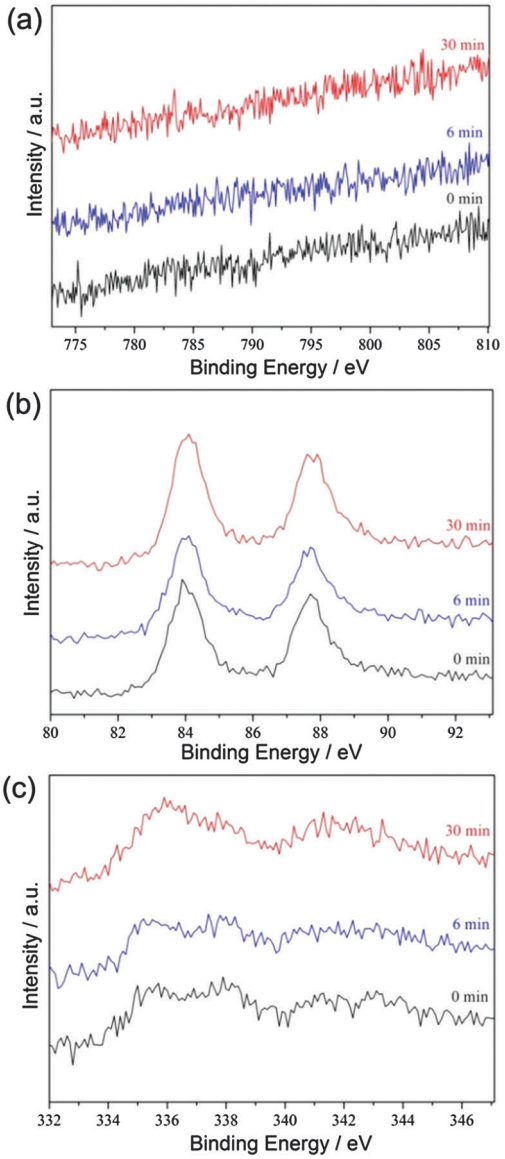

Fig. 3 (a) Co 2p, (b) Au 4f, and (c) Pd 3d XPS spectra of $(Co_3)_EAu_{0.6}Pd_{0.4}$/rGO after argon sputtering for 0, 6 and 30 min.

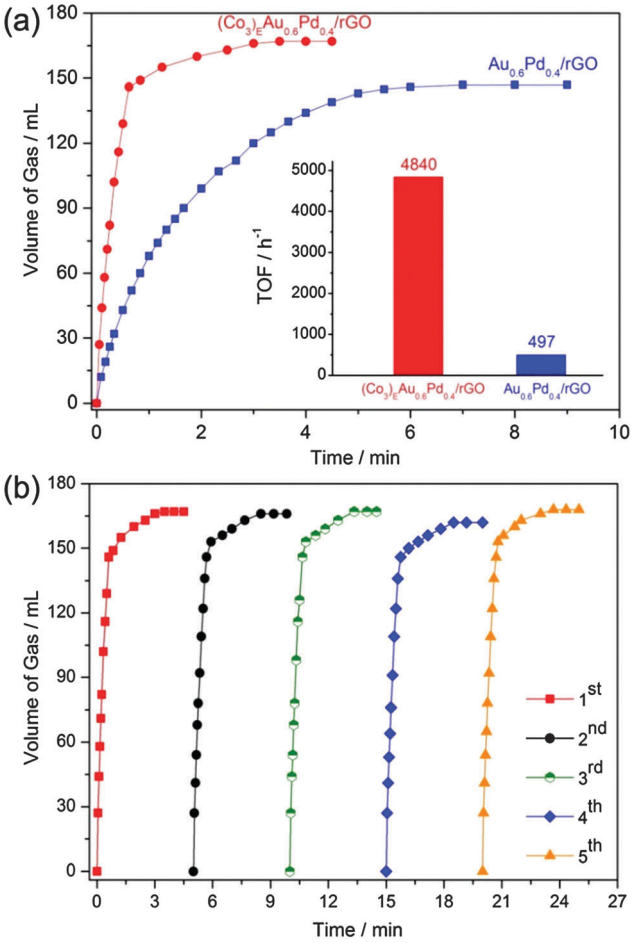

Fig. 4 (a) Volume of the generated gas (H_2 + CO_2) *versus* time for the dehydrogenation of FA over the $(Co_3)_EAu_{0.6}Pd_{0.4}$/rGO and $Au_{0.6}Pd_{0.4}$/rGO catalysts (inset: the corresponding TOF values) and (b) durability test for the dehydrogenation of FA over $(Co_3)_EAu_{0.6}Pd_{0.4}$/rGO (n_{AuPd}/n_{FA} = 0.02, n_{SF}/n_{FA} = 2.5, 323 K).

of FA with the release of 146 mL gas of H_2 + CO_2 in 0.62 min (n_{AuPd}/n_{FA} = 0.02 and n_{SF}/n_{FA} = 2.5) at 323 K, giving a TOF as high as 4840 h^{-1} (Fig. S9, ESI†), the highest value reported thus far (Table S1, ESI†).[7] After that, the generated gas with a slow speed is attributed to the decomposition of SF. The catalytic activities of the $(Co_3)_EAu_{0.6}Pd_{0.4}$/rGO catalysts with lower metal loadings have not shown significant changes (Fig. S10, ESI†).

Gas chromatography (GC) measurements demonstrate that the produced gas consists of H_2 and CO_2 without a trace of CO (below 5 ppm), implying that the as-synthesized $(CO_3)_EAu_{0.6}Pd_{0.4}$/rGO catalyst has a high selectivity for the dehydrogenation of FA into H_2 and CO_2 (Fig. S11, ESI†). Such excellent catalytic performance for FA dehydrogenation can meet the requirements of practical applications. Herein, it should be noted that the molar ratio of SF/FA has an obvious influence on the gas release rate (Fig. S12, ESI†). The gas release rate increases rapidly until the molar ratio of SF/FA increases up to 2.5. The further increase, however, makes no actual impression on the FA decomposition. On the other hand, the catalytic performance of $(Co_3)_EAu_yPd_{1-y}$/rGO is affected by the molar ratio of Au/Pd (Fig. S13, ESI†). The mono-metallic $(Co_3)_EAu$/rGO has no activity while $(Co_3)_EPd$/rGO has a low activity. However, the introduction of Au to Pd leads to a dramatically enhanced efficiency, which reaches its best value at n_{Au}/n_{Pd} = 6/4, indicative of the excellent synergistic effects between Au and Pd for FA decomposition.[12] Additionally, rGO is an excellent support for the catalysis, which is demonstrated by the quite low activities of their support-free counterparts (Fig. S14, ESI†).

Further, the increased hydrogen release rates from the FA/SF systems have been observed at elevated temperatures (Fig. S15, ESI†). The activation energy (E_a) in this process is calculated to be 39.77 kJ mol^{-1}, which is lower than most of the reported heterogeneous and homogeneous systems for FA dehydrogenation.[5,6d,7,13] After the catalytic reaction, the catalyst was recollected by centrifugation, washed with water and recycled for further use. As shown in Fig. 4b and Table S2 (ESI†), no significant loss in activity was observed over five cycles. The structure and

size distribution of metal NPs after the catalytic reactions have been found to be identical to those of the pristine catalyst (Fig. S16 and S17, ESI†). In contrast, the CO poisoned $(Co_3)_EAu_{0.6}Pd_{0.4}$/rGO, prepared by exposing the catalyst to a CO atmosphere showed no catalytic activity (Fig. S18, ESI†). It is clear that the $(Co_3)_EAu_{0.6}Pd_{0.4}$/rGO catalyst possesses high selectivity, durability and stability during the FA dehydrogenation.

In conclusion, a $(Co_3)_EAu_{0.6}Pd_{0.4}$/rGO catalyst has been synthesized using a simple non-noble metal sacrificial method. The obtained catalyst shows efficient catalytic activity for hydrogen generation from the FA/SF system with the highest TOF of 4840 h^{-1} at 323 K and possesses high selectivity, durability and stability over 5 cycles. It is believed that the way to the utilization of FA as a hydrogen carrier will be paved by the practical use of the presently provided catalyst.

The authors thank Dr Takeyuki Uchida for TEM measurements, and METI, AIST and Kobe University for financial support. X. C. Yang is grateful to the China Scholarship Council (CSC) and Ministry of Education, Culture, Sports, Science and Technology-Japan (MEXT) for a PhD scholarship.

Notes and references

1 (*a*) L. Schlapbach and A. Züttel, *Nature*, 2001, **414**, 353; (*b*) P. E. de Jongh, *Nat. Mater.*, 2011, **10**, 265; (*c*) A. Boddien, C. Federsel, P. Sponholz, D. Mellmann, R. Jackstell, H. Junge, G. Laurenczy and M. Beller, *Energy Environ. Sci.*, 2012, **5**, 8907.

2 (*a*) M. Grasemann and G. Laurenczy, *Energy Environ. Sci.*, 2012, **5**, 8171; (*b*) A. F. Dalebrook, W. Gan, M. Grasemann, S. Moret and G. Laurenczy, *Chem. Commun.*, 2013, **49**, 8735.

3 (*a*) M. Yadav and Q. Xu, *Energy Environ. Sci.*, 2012, **5**, 9698; (*b*) Q. Y. Bi, J. D. Lin, Y. M. Liu, X. L. Du, J. Q. Wang, H. Y. He and Y. Cao, *Angew. Chem., Int. Ed.*, 2014, **53**, 13583.

4 (*a*) S. Fukuzumi, T. Kobayashi and T. Suenobu, *J. Am. Chem. Soc.*, 2010, **132**, 1496; (*b*) Z. L. Wang, J. M. Yan, H. L. Wang, Y. Ping and Q. Jiang, *J. Mater. Chem. A*, 2013, **1**, 12721.

5 (*a*) C. Fellay, P. J. Dyson and G. Laurenczy, *Angew. Chem., Int. Ed.*, 2008, **47**, 3966; (*b*) Y. Himeda, *Green Chem.*, 2009, **11**, 2018; (*c*) A. Boddien, B. Loges, F. Gartner, C. Torborg, K. Fumino, H. Junge, R. Ludwig and M. Beller, *J. Am. Chem. Soc.*, 2010, **132**, 8924; (*d*) A. Boddien, D. Mellmann, F. Gärtner, R. Jackstell, H. Junge, P. J. Dyson, G. Laurenczy, R. Ludwig and M. Beller, *Science*, 2011, **333**, 1733; (*e*) Z. L. Wang, J. M. Yan, Y. Ping, H. L. Wang, W. T. Zheng and Q. Jiang, *Angew. Chem., Int. Ed.*, 2013, **52**, 4406; (*f*) D. Mellmann, E. Barsch, M. Bauer, K. Grabow, A. Boddien, A. Kammer, P. Sponholz, U. Bentrup, R. Jackstell, H. Junge, G. Laurenczy, R. Ludwig and M. Beller, *Chem. – Eur. J.*, 2014, **20**, 13589; (*g*) S. J. Li, Y. Ping, J. M. Yan, H. L. Wang, M. Wu and Q. Jiang, *J. Mater. Chem. A*, 2015, **3**, 14535.

6 (*a*) D. A. Bulushev, S. Beloshapkin and J. R. H. Ross, *Catal. Today*, 2010, **154**, 7; (*b*) D. R. Dreyer, S. J. Park, C. W. Bielawski and R. S. Ruoff, *Chem. Soc. Rev.*, 2010, **39**, 228; (*c*) K. Tedsree, T. Li, S. Jones, C. W. A. Chan, K. M. K. Yu, P. A. J. Bagot, E. A. Marquis, G. D. W. Smith and S. C. E. Tsang, *Nat. Nanotechnol.*, 2011, **6**, 302; (*d*) X. J. Gu, Z. H. Lu, H. L. Jiang, T. Akita and Q. Xu, *J. Am. Chem. Soc.*, 2011, **133**, 11822; (*e*) Q. Y. Bi, X. L. Du, Y. M. Liu, Y. Cao, H. Y. He and K. N. Fan, *J. Am. Chem. Soc.*, 2012, **134**, 8926; (*f*) N. Yi, H. Saltsburg and M. Flytzani-Stephanopoulos, *ChemSusChem*, 2013, **6**, 816; (*g*) K. Mori, M. Dojo and H. Yamashita, *ACS Catal.*, 2013, **3**, 1114; (*h*) Z. L. Wang, Y. Ping, J. M. Yan, H. L. Wang and Q. Jiang, *Int. J. Hydrogen Energy*, 2014, **39**, 4850; (*i*) Q. L. Zhu, N. Tsumori and Q. Xu, *Chem. Sci.*, 2014, **5**, 195; (*j*) Q. L. Zhu and Q. Xu, *Energy Environ. Sci.*, 2015, **8**, 478; (*k*) K. Mandal, D. Bhattacharjee and S. Dasgupta, *Int. J. Hydrogen Energy*, 2015, **40**, 4786; (*l*) S. Wu, F. Yang, H. Wang, R. Chen, P. C. Sun and T. H. Chen, *Chem. Commun.*, 2015, **51**, 10887; (*m*) M. Hattor, H. Einaga, T. Daioc and M. Tsuji, *J. Mater. Chem. A*, 2015, **3**, 4453; (*n*) A. Bulut, M. Yurderi, Y. Karatas, M. Zahmakiran, H. Kivrak, M. Gulcan and M. Kaya, *Appl. Catal., B*, 2015, **164**, 324.

7 (*a*) J. M. Yan, Z. L. Wang, L. Gu, S. J. Li, H. L. Wang, W. T. Zheng and Q. Jiang, *Adv. Energy Mater.*, 2015, **5**, 1500107; (*b*) Y. Chen, Q. L. Zhu, N. Tsumori and Q. Xu, *J. Am. Chem. Soc.*, 2015, **137**, 106; (*c*) Q. G. Liu, X. F. Yang, Y. Q. Huang, S. T. Xu, X. Su, X. L. Pan, J. M. Xu, A. Q. Wang, C. H. Liang, X. K. Wang and T. Zhang, *Energy Environ. Sci.*, 2015, **8**, 3207; (*d*) F. Z. Song, Q. L. Zhu, N. Tsumori and Q. Xu, *ACS Catal.*, 2015, **5**, 5141.

8 G. N. Glavee, K. J. Klabunde, C. M. Sorensen and G. C. Hadjapnayis, *Langmuir*, 1992, **8**, 771.

9 (*a*) W. S. Hummers and R. E. Offeman, *J. Am. Chem. Soc.*, 1958, **80**, 1339; (*b*) Y. Chen, X. Zhang, P. Xu and Y. Ma, *Chem. Commun.*, 2009, 4527.

10 (*a*) T. García, S. Agouram, A. Dejoz, J. F. Sánchez-Royo, L. Torrente-Murciano and B. Solsona, *Catal. Today*, 2015, **248**, 48; (*b*) C. C. Han, L. N. Wu, L. Ge, Y. J. Li and Z. Zhao, *Carbon*, 2015, **92**, 32.

11 (*a*) F. Ye, X. Cao, L. Yu, S. Chen and W. Lin, *Int. J. Electrochem. Sci.*, 2012, **7**, 1251; (*b*) Z. Huang, S. Wang, J. Wang, Y. Yu, J. Wen and R. Li, *Electrochim. Acta*, 2015, **152**, 117.

12 (*a*) B. Pawelec, E. Cano-Serrano, J. M. Campos-Martin, R. M. Navarro, S. Thomas and J. L. G. Fierro, *Appl. Catal., A*, 2004, **275**, 127; (*b*) T. Déronzier, F. Morfin, M. Lomello and J. L. Rousset, *J. Catal.*, 2014, **311**, 221.

13 (*a*) X. Zhou, Y. Huang, W. Xing, C. Liu, J. Liao and T. Lu, *Chem. Commun.*, 2008, 3540; (*b*) D. A. Bulushev, L. Jia, S. Beloshapkin and J. R. H. Ross, *Chem. Commun.*, 2012, **48**, 4184.

